Self-Assembly in Solution of Block Copolymers with Annealing Polyelectrolyte Blocks

E. B. Zhulina[†,‡] and O. V. Borisov*[,†,§]

Institute of Macromolecular Compounds of the Russian Academy of Sciences, 199004, St. Petersburg, Russia; Department of Chemistry and Biochemistry and Center for Polymer Research, The University of Texas at Austin, Austin, Texas 78712; and LRMP/UMR 5067, Helioparc Pau-Pyrenees, 64053 Pau, France

Received June 4, 2002; Revised Manuscript Received August 8, 2002

ABSTRACT: A theory describing the self-assembly of diblock copolymers with a weak (annealing) polyelectrolyte block and a hydrophobic block is developed. Copolymers with short hydrophobic and long polyelectrolyte block form starlike micelles in aqueous solution; otherwise, crew-cut micelles are found. We demonstrate that there is strong coupling between copolymer self-assembly and ionization of the polyelectrolyte block. At low pH and/or low salt concentration large quasi-neutral micelles with nondissociated coronae are stable. An increase in salt concentration promotes ionization of coronae and leads to the decrease in aggregation number. The structural rearrangement occurs continuously for crew-cut micelles while for starlike micelles the jump-wise morphological transition is predicted. A subsequent increase in salt concentration results in increasing aggregation number accompanied by weak decrease in the corona span. An increase in pH leads to decreasing aggregation number and increasing span of the corona; this rearrangements occur continuously or (in the case of starlike micelles) discontinuously. The phase diagrams of the micellar solution in salt concentration−pH coordinates are obtained. The exponents for the corresponding power law dependences and cmc are calculated in the mean-field approximation.

1. Introduction

Block copolymers comprising polyelectrolyte and hydrophobic blocks (or hydrophobically end-modified polyelectrolytes) are capable of self-assembly in solutions and at interfaces, giving rise to micellar-like aggregates or interfacial monolayers. These systems were extensively studied experimentally during recent years[1−8] because of their relevance for colloid stabilization in polar solvents, design of nanoreactors, and drug-delivery systems.[9−12] The appearance of spherical micelles with a dense hydrophobic core and extended charged corona was detected by light and small-angle neutron scattering (SANS) experiments in solutions of diblock copolymers with a long polyelectrolye block and a short hydrophobic (aliphatic) block.

Numerous experiments were performed on copolymers with partially sulfonated polystyrene (PS/PSS) block. Because of large dissociation constant of PSS, all the sulfonated monomers are ionized in water solution irrespective of the ionic strength or pH. As a result, the fraction of charged monomers in the PS/PSS block is "quenched" and equal to the fraction of sulfonated monomers in the PS/PSS block of nonassociated copolymer. Typically, PS/PSS blocks with high degree of sulfonation were used to ensure the solubility of block copolymer in water. (At lower degree of sulfonation, PS/PSS is insoluble due to the hydrophobic nature of styrene monomers.)

The equilibrium structure of charged micelles in salt-free solutions was analyzed in a number of theoretical studies.[13−16] In our recent work[17] we explored systematically the effects of the ionic strength in the solution on the thermodynamics of micellization of copolymers with a hydrophobic and a quenched polyelectrolyte block. We demonstrated that an increase in the ionic strength results in the increase in the aggregation number and, simultaneously, in a weak decrease in the dimensions of the micellar coronae due to enhancing screening of the Coulomb interactions between the corona blocks. Our analysis in ref 17 was based on the scaling arguments and enabled us to extrapolate the results for the high salt limit to the quasi-neutral behavior described by the scaling theory of neutral block copolymer micelles.[18,19] The predicted exponent for the power law dependence of micelle size as a function of the salt concentration was confirmed by recent observations of Förster et al.[8]

In another set of experiments the poly(acrylic acid) was used as a polyelectrolyte block.[7] In contrast to sulfonic acid, acrylic (or methacrylic) acid is weakly dissociating (p$K \approx 4.7$), and the degree of dissociation of acidic monomers depends strongly on the local pH. Most of experiments deal with PAA at sufficiently high pH > pK. Under these conditions, the degree of ionization of PAA block is close to unity for both associated in micelles and free block copolymer molecules. In this situation the theoretical predictions for micelles with quenched polyelectrolyte corona blocks still apply. However, the situation is expected to be qualitatively different in the solution of lower pH ∼ pK. As was demonstrated in refs 20−22 and later confirmed experimentally,[23,24] the degree of dissociation of weak polyelectrolyte chains in polyelectrolyte brushes and starlike polyelectrolytes is significantly lower than in the bulk of a salt-free solution. The ionization is suppressed due to higher local concentration of counterions (H^+ ions) "trapped" inside many-arm stars and brushes. Hence, aggregation of the block copolymer chains into micelles would affect their degree of dissociation, and strong

[†] Russian Academy of Sciences.
[‡] The University of Texas at Austin.
[§] LRMP/UMR 5067.

10.1021/ma020865s CCC: $22.00
Published on Web 10/16/2002

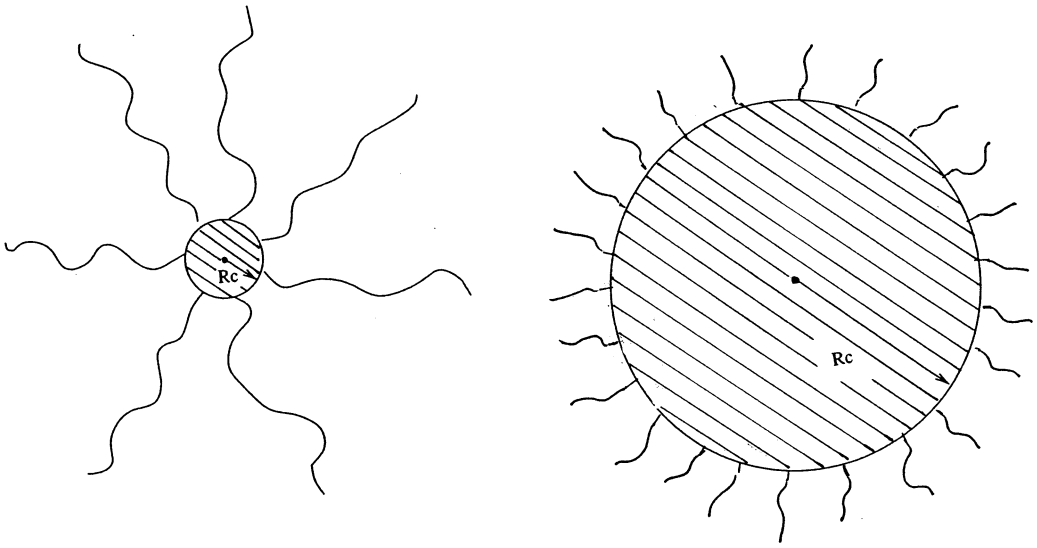

Figure 1. Starlike (a) and crew-cut (b) block copolymer micelle. $p \geq 1$ is the aggregation number, N_A is the number of monomers in the hydrophilic block, N_B is the number of monomers in the hydrophobic block, R_c is the radius of the core, and R_{corona} is the outer radius of the corona.

coupling between ionization and the chain association is expected. An addition of salt, e.g., NaCl, would lead to progressive substitution of H^+ ions by Na^+ ions in the corona of micelle, thus promoting its ionization. Therefore, the effect of salt on the self-assembly of block copolymers with weak polyelectrolyte blocks is expected to be more complicated than for copolymers with quenched polyelectrolyte blocks.

The interference between ionization and association equilibria is the key point in understanding the self-assembly of block copolymers with weak polyelectrolyte block. The goal of the present paper is a systematic study of the equilibrium properties of spherical micelles with weakly dissociating coronae. We predict that in contrast to block copolymers with quenched charges the coupling of ionization and self-assembly can lead to jump-wise rearrangements of micelles with annealing coronae. These abrupt transformations can be caused by variations in both the pH and the ionic strength in the solution and constitute the first-order phase transitions. We explore the power law dependences for structural parameters of the micelles and delineate the ranges of their thermodynamic stability.

The rest of the paper is organized as follows. In section 2 we introduce the model of micellization in solution of ionic/nonionic block copolymers; the general formalism is presented in section 3. In sections 4 and 5 we consider the structure, thermodynamics of self-assembly, and morphological transitions for starlike and for crew-cut micelles, respectively. Our conclusions are summarized in section 6.

2. Model

Consider a dilute aqueous solution of block copolymer comprising a hydrophobic block (with degree of polymerization N_B) and a weak polyacid block (with degree of polymerization N_A). Each monomer of the polyacid can be ionized via dissociation of hydrogen ion, H^+. (For polybases, ionization occurs through protonation of the monomer, and generalization of the model is straightforward.) The dissociation constant for an individual acidic monomer is K. Then the degree of dissociation of the acidic monomers in the bulk of the solution, α_b, depends on the value of pH, i.e., on the bulk concentration c_{bH^+} of H^+ ions via the equation

$$\frac{\alpha_b}{1-\alpha_b} = \frac{K}{c_{bH^+}} \tag{1}$$

In addition to block copolymer and H^+ ions, the solution contains also monovalent ions of various types, e.g., Na^+, Cl^-, OH^-, etc., due to added salt, base, or acid. The solvent (water) is modeled by a continuous medium with the dielectric permittivity ϵ. Water dissociation is accounted for by the constraint imposed on the respective bulk concentrations c_{bH^+} and c_{bOH^-} of H^+ and OH^- ions. Namely, $c_{bH^+}c_{bOH^-} = c_*^2$, where $c_* = 10^{-7}$mol/L is the concentration of H^+ and OH^- ions in pure water.

Both blocks of copolymer are assumed to be intrinsically flexible. That is, the statistical segment length is on the order of a monomer unit length a, which is taken as the unit length in our subsequent analysis. We assume also that the monomer length is on the order of the Bjerrum length, $l_B = e^2/k_BT\epsilon$ (= 0.7 nm in water under normal conditions), $l_B \simeq a$. Here, e is the elementary charge, T is the temperature, and k_B is the Boltzmann constant. The latter condition ensures that the effects of the induced electrostatic stiffening of blocks A can be safely neglected.

The short-range (van der Waals) interactions between monomers are modeled in terms of the virial expansion of the nonelectrostatic free energy. The corresponding dimensionless second, v_A and v_B, and the third, w_A and w_B, virial coefficients are normalized by the factors a^{-3} and a^{-6}, respectively. We assume that water is a poor solvent for the hydrophobic B-block so that $v_B \cong -\tau_B \equiv (\theta_B - T)/\theta_B \leq 0$, where τ_B is a relative deviation form the θ-temperature for the B-blocks. On the contrary, for monomers of a polyelectrolyte block water is assumed to be a marginal good solvent so that $v_A \geq 0$. The third virial coefficients, w_A and w_B, are virtually independent of T and are on the order of unity.

When the polymer concentration in solution exceeds the so-called critical micelle concentration (cmc), the block copolymer chains associate and form micelles. A micelle consists of the hydrophobic core comprising collapsed blocks B which is surrounded by the polyelectrolyte corona of blocks A (Figure 1). We employ the

simplest model of spherical micelle with the following features: (i) the width of the core/corona boundary is small compared to the size of the micelle, and therefore, blocks A and B are envisioned as grafted to the core interface; (ii) the corona is considered as a semidilute solution with average polymer concentration c_p (the gradient in polymer density within the corona is ignored); (iii) blocks A and B are assumed to be stretched uniformly.

The equilibrium structure of micelles is determined by the balance of the excess free energy of the water−core interface, $F_{surface}(p)$, and the free energies of the core, $F_{core}(p)$, and that of the corona, $F_{corona}(p)$, where p is the number of chains associated into the micelle. The equilibrium aggregation number p_{eq} can be found by minimizing the Gibbs free energy of the micelle

$$F(p) = F_{corona}(p) + F_{core}(p) + F_{surface}(p) \qquad (2)$$

calculated per one chain. Then the cmc can be found as

$$\ln \text{cmc} \approx (F(p_{eq}) - F(p=1))/k_BT \qquad (3)$$

3. General Formalism

3.1. Free Energy of Corona. In our analysis we consider the charged corona of a micelle as a curved polyelectrolyte brush. To calculate the free energy of the corona, we employ the combination of the mean-field and the local electroneutrality approximations. The latter one assumes that the local excess (number) density of counterions inside the corona is approximately equal to the local (number) density of charged monomers. This condition ensures the local (and the total) electroneutrality of the micellar corona. As demonstrated in refs 21 and 25−29 and also confirmed experimentally,[30] the local electroneutrality approximation is justified even in a salt-free solution provided that the number of polyelectrolyte chains in the corona is sufficiently large. In other words, because of strong Coulomb attraction to the polyelectrolyte blocks, most of the counterions are retained inside the micellar corona. When the solution contains salt ions, the local electroneutrality condition yields

$$\sum_{i^-} c_{i^-} + \alpha c_p = \sum_{i^+} c_{i^+} \qquad (4)$$

where c_p and α are the (local) concentration of monomers and the local degree of ionization in the corona, respectively The summation on the right-hand side (rhs) is running over all the cationic species (i.e., salt ions, c_{Na^+}, and hydrogen ions, c_{H^+}) while the summation on the left-hand side (lhs) is running over all the anionic species (i.e., salt ions, c_{Cl^-}, and hydroxyl ions, c_{OH^-}). The distribution of co- and counterions between the interior of corona and the bulk solution is given by the Donnan rule, which in the case of monovalent ions is formulated as

$$c_i/c_{bi^-} = c_{bi^+}/c_{i^+} = \exp(e\Delta\psi/k_BT) \qquad (5)$$

Here, subscript "b" denotes the bulk values, and $\Delta\psi$ is the difference in the electrostatic potential between the interior of the corona and the bulk solution. By combining eqs 4 and 5, one gets the following expression for the excess potential inside the corona

$$\exp(e\Delta\psi/k_BT) = \sqrt{1 + (\alpha c_p/\sum_i c_{bi})^2} - \alpha c_p/\sum_i c_{bi} = \sqrt{1 + (\alpha c_p/\Phi_{ion})^2} - \alpha c_p/\Phi_{ion} \qquad (6)$$

where $\Phi_{ion} = \sum_i c_{bi}$ is the total concentration of the ions in the bulk solution regardless of their sign. As long as the concentrations (or chemical potentials) of all the mobile ions in the bulk solution are fixed, the relevant free energy of the corona is the Gibbs free energy,

$$F_{corona}(p)/k_BT = \frac{3R_{corona}^2}{2N_A} + \nu_A N_A c_p + \frac{N_A}{c_p} f_{corona}(c_p,\{c_i\},\{c_{bi}\})/k_BT \qquad (7)$$

Here, R_{corona} is thickness of the corona, c_p is average concentration of monomers in the corona, and $f_{corona}(c_p,\{c_i\},\{c_{bi}\})$ is the polyelectrolyte contribution to the free energy of the corona (per unit volume). The first term in eq 7 accounts for the uniform stretching of blocks A with the end-to-end distance R_{corona}. The second term is the nonelectrostatic free energy of binary contacts between monomers. The last term is the polyelectrolyte part of the corona free energy where

$$f_{corona}(c_p,\{c_i\},\{c_{bi}\})/k_BT = \sum_i c_i(\ln c_i - 1) + \pi_b/k_BT - \sum_i c_i \ln c_{bi} + c_p[\alpha \ln \alpha + (1-\alpha)\ln(1-\alpha) + \alpha \ln c_{bH^+} - \alpha \ln K] \qquad (8)$$

The first term on the rhs in eq 8 is due to the translational entropy of ions in the corona per unit volume, the second term is the osmotic pressure in the bulk solution,

$$\pi_b = k_BT\sum_i c_{bi} = k_BT\Phi_{ion} \qquad (9)$$

the third term arises from the chemical potentials of ions in the bulk solution,

$$\mu_{bi} = kT \ln c_{bi} + \mu_i^0 \qquad (10)$$

(μ_i^0 are the standard chemical potentials of species i), and the summation in eqs 8 and 9 is running over all the mobile ion species. The terms in square brackets are due to ionization of corona chains. Here, the first two terms account for the mixing entropy of the charged and neutral groups on the chains, and the third term is due to hydrogen ions that were "born" in the corona, whereas the last term characterizes the "strength" of an acidic group

$$k_BT \ln K = \mu_{AH}^0 - \mu_{A^-}^0 - \mu_{H^+}^0 \qquad (11)$$

The degree of ionization of the corona chains α is obtained by minimization of the free energy of the corona, eq 8, with respect to α under the constraint of local electroneutrality (eq 4) to give

$$\frac{\alpha}{1-\alpha} = \frac{K}{c_{H^+}} \qquad (12)$$

Equation 12 can also be represented as

$$\frac{\alpha}{1-\alpha}\frac{1-\alpha_b}{\alpha_b}=\frac{c_{bH^+}}{c_{H^+}}=\exp(e\Delta\psi/k_BT) \qquad (13)$$

where α_b is the degree of dissociation of a monomer in the bulk of the solution. Remarkably, dissociation of the blocks in the corona is always smaller than that in the bulk of the solution, $\alpha \le \alpha_b$, because $c_{H^+} \ge c_{bH^+}$. (The electrostatic potential inside negatively charged corona is lower than that in the bulk of the solution.)

With the account of eqs 12, 4, 5, and 6, polyelectrolyte contribution to the free energy can be represented as

$$f_{corona}(c_p,\Phi_{ion})/k_BT=-(\sqrt{1+(\alpha c_p/\Phi_{ion})^2}-1)\Phi_{ion}+c_p\ln(1-\alpha) \qquad (14)$$

where $\alpha=\alpha(c_p,\Phi_{ion})$ is determined by eqs 13 and 6 as

$$\frac{\alpha}{1-\alpha}\frac{1-\alpha_b}{\alpha_b}=\sqrt{1+(\alpha c_p/\Phi_{ion})^2}-\alpha c_p/\Phi_{ion} \qquad (15)$$

Equations 14 and 15 can be expanded with respect to the parameter $\alpha c_p/\Phi_{ion}$, which is either large or small in the low-salt and high-salt asymptotic limits, respectively. As a result, one gets

$$\alpha \cong \begin{cases} \dfrac{\alpha_b}{1-\alpha_b}\dfrac{\Phi_{ion}}{c_p}, & \alpha c_p/\Phi_{ion} \gg 1 \\ \alpha_b\left(1-\dfrac{\alpha_b c_p}{\Phi_{ion}}(1-\alpha_b)\right), & \alpha c_p/\Phi_{ion} \ll 1 \end{cases} \qquad (16)$$

and

$$f_{corona}(c_p,\Phi_{ion})/k_BT \cong \begin{cases} -\alpha c_p + c_p\ln(1-\alpha), & \alpha c_p/\Phi_{ion} \gg 1 \\ \dfrac{\alpha_b^2 c_p^2}{2\Phi_{ion}} + c_p\ln(1-\alpha_b), & \alpha c_p/\Phi_{ion} \ll 1 \end{cases} \qquad (17)$$

As follows from eq 16, the degree of ionization of the coronal chains in the low salt limit is much smaller than that in the bulk of the solution, $\alpha \ll \alpha_b$, and monotonically increases with increasing salt concentration. In the high salt limit α asymptotically approaches the bulk value, α_b.

3.2. Free Energies of the Core and of the Interface. Under uniform extension of blocks B in the core of micelle, the elastic free energy of the core per chain yields

$$\frac{F_{core}(p)}{k_BT} \cong \frac{3R_{core}^2(p)}{2N_B} \qquad (18)$$

We note that the free energy of nonelectrostatic interactions in the collapsed core does not depend on the aggregation number p (it is determined only by the values of $v_B \simeq \tau_B$, w_B, and N_B), and we omit this contribution from further consideration. The equilibrium concentration of polymer in the core of micelle is determined by the balance of attractive pair and repulsive ternary contacts between B monomers. With accuracy of a numerical coefficient it coincides with τ_B.[31] Then radius of the core is

$$R_{core}(p) \simeq \left(\frac{3pN_B}{4\pi\tau_B}\right)^{1/3} \qquad (19)$$

The excess free energy of the core−water interface per chain is given by

$$F_{surface}(p)/k_BT=\frac{4\pi\gamma R_{core}^2}{p}\simeq\frac{3\tau_B N_B}{R_{core}} \qquad (20)$$

where $k_BT\gamma a^2 \cong k_BT\tau_B^2$ is the surface free energy per unit area at the core−water interface.

At a given polymer concentration c_p, the thickness of the corona, R_{corona}, and the radius of the core, R_{core}, of a spherical micelle are interrelated as

$$R_{corona}=R_{core}\left[\left(1+\frac{N_A\tau_B}{N_Bc_p}\right)^{1/3}-1\right] \qquad (21)$$

Equation 21 indicates that when the ratio $N_A\tau_B/N_Bc_p \gg 1$, the micelles have starlike shape with $R_{corona} \gg R_{core}$. When, however, $N_A\tau_B/N_Bc_p \ll 1$, one finds the so-called crew-cut micelles with $R_{corona} \ll R_{core}$.

3.3. Free Energy per Chain in Spherical Micelle. With the account of eqs 7, 14, 18, 20, and 21, the free energy per chain in the micelle can be represented as

$$F/k_BT \cong \frac{3R_{core}^2}{2N_B}+\frac{3R_{core}^2}{2N_A}\left[\left(1+\frac{N_A\tau_B}{N_Bc_p}\right)^{1/3}-1\right]^2+\frac{3N_B\tau_B}{R_{core}}+v_AN_Ac_p+N_A\ln(1-\alpha)-N_A\frac{\Phi_{ion}}{c_p}(\sqrt{1+(\alpha c_p/\Phi_{ion})^2}-1) \qquad (22)$$

where α is related to polymer concentration in the corona, c_p, and bulk concentration of ions, Φ_{ion}, via eq 15. Here, the first two terms account for the elastic stretching of the blocks B and A, respectively, the third term is the surface free energy of the core−water interface, and the fourth term describes the short-range binary interactions between monomers A, whereas the last two terms are due to the electrostatic interactions in the corona and translational entropy of mobile ions.

To derive the parameters of an equilibrium micelle as a function of α_b and Φ_{ion}, this free energy must be minimized with respect to R_{core} and c_p. Minimization of the free energy, eq 22, with respect to R_{core} gives the relation between R_{core} and c_p in an equilibrium micelle,

$$R_{core}=N_B^{2/3}\tau_B^{1/3}\left\{1+\frac{N_B}{N_A}\left[\left(1+\frac{N_A\tau_B}{N_Bc_p}\right)^{1/3}-1\right]^2\right\}^{-1/3} \qquad (23)$$

Using the packing condition, eq 19, we find for the aggregation number in a spherical micelle

$$p=\frac{4\pi}{3}N_B\tau_B^2\left\{1+\frac{N_B}{N_A}\left[\left(1+\frac{N_A\tau_B}{N_Bc_p}\right)^{1/3}-1\right]^2\right\}^{-1} \qquad (24)$$

By substituting eq 23 in eq 22, we find

$$\frac{F}{N_Ak_BT}\cong\frac{9\tau_B^{2/3}N_B^{1/3}}{2N_A}\left\{1+\frac{N_B}{N_A}\left[\left(1+\frac{N_A\tau_B}{N_Bc_p}\right)^{1/3}-1\right]^2\right\}^{1/3}+v_Ac_p+\ln(1-\alpha)-\frac{\Phi_{ion}}{c_p}(\sqrt{1+(\alpha c_p/\Phi_{ion})^2}-1) \qquad (25)$$

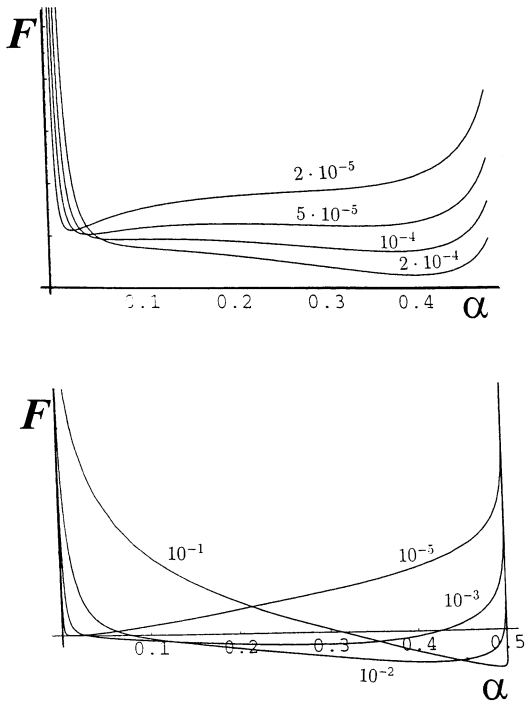

Figure 2. Free energy per chain in a starlike (a) and crew-cut (b) micelle as a function of the degree of ionization of the coronal chains for different salt concentrations; $\alpha_b = 0.5$.

where α is still related to c_p through eq 15. Equation 25 determines the free energy of a micelle (per A-monomer) as a function of c_p or, alternatively, as a function of α. If N_A, N_B, τ_B, and v_A are fixed, the variable external parameters are Φ_{ion} and α_b (we remark that the latter one depends on c_{bH^+}, i.e., on pH in the solution).

Figure 2 demonstrates typical behavior of $F/N_A k_B T$ as a function of α (eq 25) for starlike micelles (a) and crew-cut micelles (b) at various bulk concentrations of added ions Φ_{ion}. When insoluble block B is relatively short (Figure 2a), the shape of the $F/N_A k_B T$ vs α curve essentially depends on Φ_{ion}. At very low concentrations of added ions $F/N_A k_B T$ has a single minimum located at small values of α. In this range of Φ_{ion} the micelles are relatively large and are "quasi-neutral" (ionization of the corona is suppressed, $\alpha \ll \alpha_b$). As Φ_{ion} increases, the second minimum (the metastable state) appears at relatively large values of α. This minimum corresponds to noticeably charged micelles with $\alpha \leq \alpha_b$. The two minima coexist only in a narrow range of salt concentrations, and further increase in Φ_{ion} leads to disappearance of the first minimum and progressive shift of the second minimum to values of $\alpha \simeq \alpha_b$. The behavior of $F/N_A k_B T$ in Figure 2a clearly indicates that an increase in Φ_{ion} leads to an abrupt transformation of a quasi-neutral micelle with $\alpha \ll \alpha_b$ into a charged micelle with $\alpha \approx \alpha_b$. When the insoluble block B is relatively large (Figure 2b), the $F/N_A k_B T$ vs α curve has only one minimum that shifts progressively to larger values of α as bulk concentration of ions, Φ_{ion}, increases. Such micelles rearrange continuously without abrupt transformations.

We now analyze the scaling dependences for the equilibrium parameters of starlike and crew-cut micelles under various conditions in the bulk solution.

4. Starlike Micelles

Starlike polyelectrolyte micelles with $R_{corona} \gg R_{core}$ are formed by asymmetric copolymers with short hydrophobic and long polyelectrolyte block. In this section we assume that the copolymer chains are strongly asymmetric

$$\frac{N_B}{N_A^{7/5} v_A^{3/5} \tau_B^{1/5}} \ll 1$$

and form starlike micelles in the whole range of salt concentrations, including the quasi-neutral (low/high salt) regimes. By expanding the free energy of micelle, eq 25, with respect to the parameter $N_B c_p / N_A \tau_B \ll 1$ and retaining the major term of the expansion, we find that for starlike micelles

$$F/N_A k_B T \cong \left(\frac{N_B \tau_B^2}{N_A^{5/2}}\right)^{4/9} c_p^{-2/9} + v_A c_p + \ln(1-\alpha) - \frac{\Phi_{ion}}{c_p}\left(\sqrt{1 + (\alpha c_p/\Phi_{ion})^2} - 1\right) \quad (26)$$

4.1. Quasi-Neutral Micelles. We start the analysis with the low salt limit, when the chains in the equilibrium micelles are weakly ionized, $\alpha \ll \alpha_b$. Then using the low salt asymptotics of eq 17, we can represent the free energy in eq 26 as

$$F/N_A k_B T \cong -\alpha + \ln(1-\alpha) + v_A c_p + \left(\frac{N_B \tau_B^2}{N_A^{5/2}}\right)^{4/9} c_p^{-2/9} \quad (27)$$

or, using eq 16, as

$$F(\alpha)/N_A k_B T \cong -2\alpha + v_A \frac{\alpha_b}{1-\alpha_b}\frac{\Phi_{ion}}{\alpha^2} + \frac{1-\alpha_b}{\alpha_b}\frac{N_B^2 \tau_B^4}{N_A^5 \Phi_{ion}}^{2/9} \alpha^{4/9}, \quad \alpha \ll \alpha_b \quad (28)$$

At low salt concentration the free energy exhibits a minimum corresponding to the balance of the second and the third terms in eq 28. This minimum corresponds to quasi-neutral micelles (low degree of ionization of the corona, the excluded-volume repulsion in the corona is balanced with the excess free energy of core interface). The parameters of the equilibrium quasi-neutral starlike micelles are

$$\alpha \cong \left(\frac{\alpha_b \Phi_{ion}}{1-\alpha_b}\right)^{1/2} \frac{N_A^{5/11} v_A^{9/22}}{(N_B \tau_B^2)^{2/11}} \quad (29)$$

$$p_{eq} \cong \frac{(N_B \tau_B^2)^{10/11}}{v_A^{6/11} N_A^{3/11}} \quad (30)$$

$$R_{corona} \cong N_A^{3/5} v^{1/5} p^{1/5} \cong N_A^{6/11} v_A^{1/11} (N_B \tau_B^2)^{2/11} \quad (31)$$

$$R_{core} \cong \frac{N_B^{7/11} \tau_B^{3/11}}{v_A^{2/11} N_A^{1/11}} \quad (32)$$

The corresponding free energy is given by

$$F/N_A k_B T \cong \nu_A^{2/11}\left(\frac{N_B \tau_B^2}{N_A^{5/2}}\right)^{4/11}, \quad \alpha \ll \alpha_b \qquad (33)$$

4.1.1. Cmc for Quasi-Neutral Starlike Micelles. The critical micelle concentration (cmc) is determined by eq 3. Equation 33 provides the free energy per chain $F(p_{eq})$ in the equilibrium quasi-neutral micelle,

$$F(p_{eq})/k_B T \simeq N_A^{1/11} \nu_A^{2/11} (N_B \tau_B^2)^{4/11} \qquad (34)$$

As noted earlier, ionization of chains in the corona of such micelle is suppressed ($\alpha \ll \alpha_b$) because of the lower local pH in the corona. However, the degree of ionization of a single block copolymer chain in the bulk solution is $\alpha = \alpha_b$. With accuracy of a numerical coefficient, the corresponding free energy of such a chain yields

$$F(p=1)/k_B T \cong N_B^{2/3} \tau_B^{4/3} + N_A \ln(1 - \alpha_b) \qquad (35)$$

where the two terms are the surface free energy of a collapsed block B and the dominant contribution to the free energy of the ionization of the polyelectrolyte block A, respectively. (The contributions due to the stretching of block A and the intrachain repulsive interactions can be neglected with respect to the last term on the rhs in eq 35.)

The cmc is then given by

$$\ln \mathrm{cmc}_{qn} \approx \ln \mathrm{cmc}_n - N_A \ln(1 - \alpha_b) \approx -N_B^{2/3} \tau_B^{4/3} - N_A \ln(1 - \alpha_b) \qquad (36)$$

where subscript "qn" indicates the quasi-neutral state of the polyelectrolyte micelle and

$$\ln \mathrm{cmc}_n \cong N_A^{1/11} \nu_A^{2/11} (N_B \tau_B^2)^{4/11} - N_B^{2/3} \tau_B^{4/3} \qquad (37)$$

is the critical micelle concentration for an equivalent neutral block copolymer with same lengths of blocks, N_A and N_B, under similar solvent conditions. Equation 36 demonstrates that the cmc for quasi-neutral starlike micelles is strongly affected by the value of α_b. When $-N_A \ln(1 - \alpha_b) > N_B^{2/3} \tau_B^{4/3}$, quasi-neutral micelles do not form at any concentrations of polymer in the solution ($\mathrm{cmc}_{qn} > 1$).When $-N_A \ln(1 - \alpha_b) < N_B^{2/3} \tau_B^{4/3}$, the critical micelle concentration for quasi-neutral (i.e., nonionized) polyelectrolyte micelles can be evaluated (for $\alpha_b \ll 1$) as

$$\ln \mathrm{cmc}_{qn} \approx \ln \mathrm{cmc}_n + N_A \alpha_b \qquad (38)$$

4.2. Charged Micelles. As indicated by Figure 2a, at a certain concentration of salt ions Φ_{ion} the quasi-neutral micelles rearrange into highly ionized micelles with $\alpha \approx \alpha_b$. Here, $\alpha c_p/\Phi_{ion} \ll 1$, and expansions 16 and 17 provide the following expression for the free energy of the "charged" micelle,

$$F(c_p)/N_A k_B T \cong \ln(1 - \alpha_b) + c_p\left(\nu_A + \frac{\alpha_b^2}{\Phi_{ion}}\right) + \left(\frac{N_B \tau_B^2}{N_A^{5/2}}\right)^{4/9} c_p^{-2/9} \qquad (39)$$

Apart from the term $\ln(1 - \alpha_b)$, this free energy is similar to that for a neutral starlike micelle with the second virial coefficient ν_A substituted by an effective salt-dependent second virial coefficient $\nu_{eff} = \nu_A + \alpha_b^2/\Phi_{ion}$. The minimum of the free energy, eq 39, corresponds to the balance between the binary repulsive interactions in the micellar corona (renormalized due to the additional electrostatic contribution) and the excess free energy of the core interface. The characteristics of the equilibrium micelle are given by

$$p_{eq} \cong \frac{(N_B \tau_B^2)^{10/11}}{(\nu_A + \alpha_b^2/\Phi_{ion})^{6/11} N_A^{3/11}} \qquad (40)$$

$$R_{corona} \cong N_A^{3/5}\left(\nu_A + \frac{\alpha_b^2}{\Phi_{ion}}\right)^{1/5} p^{1/5} \cong N_A^{6/11}\left(\nu_A + \frac{\alpha_b^2}{\Phi_{ion}}\right)^{1/11} (N_B \tau_B^2)^{2/11} \qquad (41)$$

$$R_{core} \cong \frac{N_B^{7/11} \tau_B^{3/11}}{(\nu_A + \alpha_b^2/\Phi_{ion})^{2/11} N_A^{1/11}} \qquad (42)$$

The free energy in equilibrium micelle yields

$$F/N_A k_B T \cong \ln(1 - \alpha_b) + (\nu_A + \alpha_b^2/\Phi_{ion})^{2/11}\left(\frac{N_B \tau_B^2}{N_A^{5/2}}\right)^{4/11}, \quad \alpha \approx \alpha_b \qquad (43)$$

4.2.1. Cmc for Charged Starlike Micelles. Equations 3, 35, and 43 give for the critical micelle concentration

$$\ln(\mathrm{cmc})_{ch} \simeq N_A^{1/11} (\nu_A + \alpha_b^2/\Phi_{ion})^{2/11} (N_B \tau_B^2)^{4/11} - N_B^{2/3} \tau_B^{4/3} = \ln(\mathrm{cmc})_n + N_A^{1/11}[(\nu_A + \alpha_b^2/\Phi_{ion})^{2/11} - \nu_A^{2/11}](N_B \tau_B^2)^{4/11} \qquad (44)$$

where the subscript "ch" indicates the charged state of starlike micelles. As follows from eq 44, the charged starlike micelles could form in the bulk solution (i.e., $\ln \mathrm{cmc}_{ch} < 0$) only if the concentration of added ions Φ_{ion} exceeds certain critical concentration Φ_{ion}^0. By setting $\ln \mathrm{cmc}_{ch} = 0$ in eq 44, we find

$$\nu_A + \frac{\alpha_b^2}{\Phi_{ion}^0} \cong \nu_0 \equiv \frac{(N_B \tau_B^2)^{5/3}}{N_A^{1/2}} \qquad (45)$$

and eq 44 can be represented as

$$\ln \mathrm{cmc}_{ch} \approx \ln \mathrm{cmc}_n\left[1 - \left(\frac{\nu_{eff}}{\nu_0}\right)^{2/11} \frac{1 - (\nu_A/\nu_{eff})^{2/11}}{1 - (\nu_A/\nu_0)^{2/11}}\right] \qquad (46)$$

When $\Phi_{ion} \gg \Phi_{ion}^0$ (or $\nu_{eff} \ll \nu_0$), the $(\mathrm{cmc})_{ch}$ approaches the $(\mathrm{cmc})_n$, the critical micelle concentration for an equivalent neutral block copolymer.

4.3. Transition Quasi-Neutral−Charged Micelles. As indicated by Figure 2, the rearrangement of quasi-neutral starlike micelles into highly charged micelles occurs abruptly (as the first-order phase transition) at certain value of the salt concentration Φ_{ion}^*. Charged micelles are unstable at $\Phi_{ion} \le \Phi_{ion}^0$ and metastable at $\Phi_{ion}^0 \le \Phi_{ion} \le \Phi_{ion}^*$. In a narrow range of salt concentrations around Φ_{ion}^* large quasi-neutral micelles coexist with smaller charged ones. The transition takes place

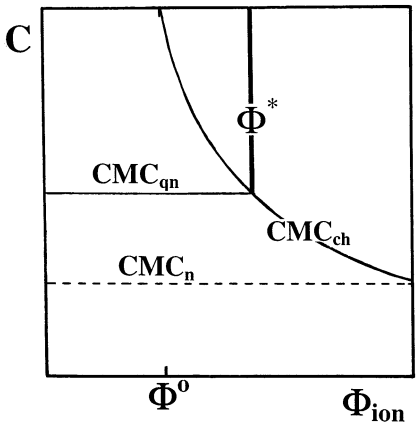

Figure 3. Diagram of states for starlike micelles in C, Φ_{ion} coordinates. The cmc's for neutral, quasi-neutral, and charged micelles are indicated; Φ^*_{ion} denotes the line of the first-order phase transition between quasi-neutral and charged micelles which occurs at $C \geq cmc_{qn}$ upon an increase in the bulk salt concentration.

when the two minima of the free energy given by eqs 33 and 43 are equally deep. By expanding $\ln(1 - \alpha_b) \approx -\alpha_b$ in eq 43, we find that the transition point v^*_{eff} is specified as

$$\alpha_b \cong [v^{*2/11}_{eff} - v^{2/11}_A]\left(\frac{N_B\tau_B^2}{N_A^{5/2}}\right)^{4/11} \quad (47)$$

In the considered range of Φ_{ion}, $v_{eff} = v_A + \alpha_b^2/\Phi_{ion} \gg v_A$, and the last term on rhs in eq 47 term can be safely neglected. As a result, we find for the transition value of salt concentration

$$\Phi^*_{ion} \cong \alpha_b^{-7/2}\left(\frac{N_B\tau_B^2}{N_A^{5/2}}\right)^2 \quad (48)$$

The rearrangement of micelles is accompanied by an abrupt decrease in the aggregation number. In the transition point, $\Phi_{ion} = \Phi^*_{ion}$, the ratio

$$\frac{p_{qn}}{p_{ch}} \simeq \left(1 + \frac{\alpha_b^2}{v_A\Phi^*_{ion}}\right)^{6/11} \gg 1 \quad (49)$$

where subscripts "ch" and "qn" indicate the quasi-neutral and the charged states of the micelle. Subsequent increase in salt concentration ($\Phi_{ion} > \Phi^*_{ion}$) leads to progressive increase in p according to eq 40.

Figure 3 demonstrates schematically the location of the transition line Φ^*_{ion} and the critical micelle concentrations, cmc_{qn} and cmc_{ch}, in the C, Φ_{ion} plane (C is the concentration of block copolymer in the solution). When polymer concentration $C < cmc_{qn}$, micelles do not form in the range of Φ_{ion} to the left of the cmc_{ch} line. As the cmc_{ch} line is intersected, the charged starlike micelles appear in the solution.

When polymer concentration $C > cmc_{qn}$, quasi-neutral micelles are found in the range of low Φ_{ion}. At the transition concentration $\Phi_{ion} = \Phi^*_{ion}$, these micelles abruptly rearrange into smaller but stronger charged micelles that progressively increase in size as Φ_{ion} increases. Alternatively, the decomposition of large quasi-neutral micelles into smaller charged ones (crossing of the $\Phi^*_{ion}(\alpha_b)$ line may be induced by an increase in pH (i.e., in α_b). Subsequent increase in pH leads to continuous decrease in the aggregation number and increase in the span of the corona.

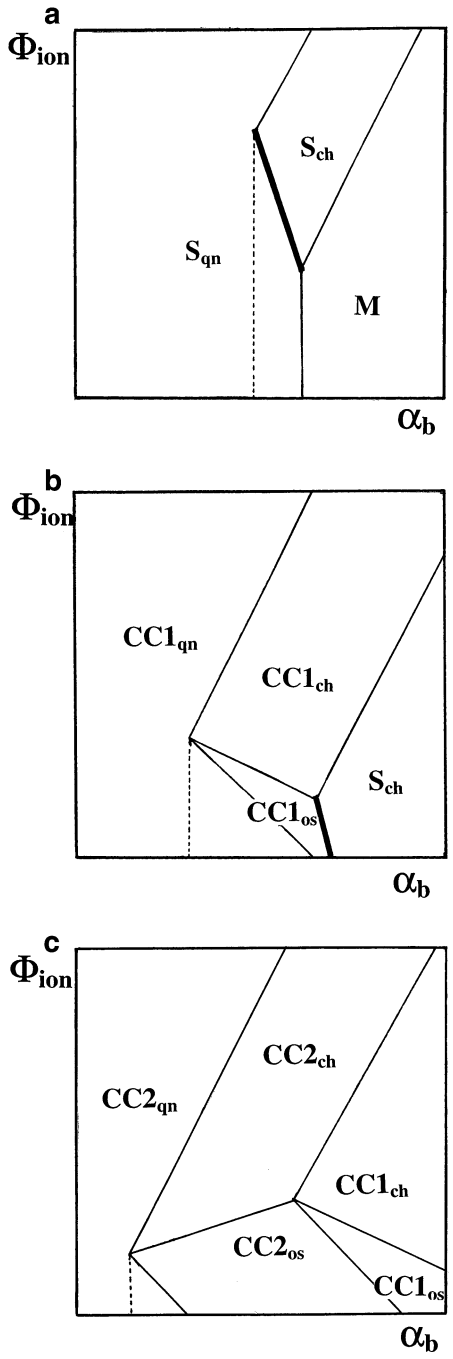

Figure 4. Diagram of states for starlike (a) crew-cut-1 (b) and crew-cut-2 (c) micelles in Φ_{ion}, α_b coordinates. The bold lines indicate the lines of the first-order phase transitions between quasi-neutral and charged star like micelles (a) or between osmotic annealing crew-cut-1 and charged starlike micelles (b). The equations for the boudaries between the regions are presented in Table 3.

Figure 4a demonstrates the diagram of the states of starlike micelles in the Φ_{ion}, α_b coordinates. We delineate four regions denoted as S_{qn}, $S_{qn'}$, S_{ch}, and M. In region S_{qn}, the starlike micelles are quasi-neutral, and their structural parameters are given by eqs 29−32. The dashed line divides region S_{qn} in two parts. To the left of the dashed line, the cmc_{qn} is virtually unaffected by the polyelectrolyte nature of the corona chains (it coincides with cmc for equivalent neutral copolymer).

Table 1. Parameters of Equilibrium Spherical Micelles

regions	p	α	R_{core}	R_{corona}
S_{qn}	$(N_B\tau_B^2)^{10/11}/\nu_A^{6/11}N_A^{3/11}$	$[(\alpha_b\Phi_{ion}/(1-\alpha_b)]^{1/2} \times [N_A^{5/11}\nu_A^{9/22}/(N_B\tau_B^2)^{2/11}]$	$N_B^{7/11}\tau_B^{3/11}/\nu_A^{2/11}N_A^{1/11}$	$N_A^{6/11}\nu_A^{1/11}(N_B\tau_B^2)^{2/11}$
S_{ch}	$(N_B\tau_B^2)^{10/11}/N_A^{3/11}\nu_{eff}^{6/11}$	α_b	$N_B^{7/11}\tau_B^{3/11}/\nu_{eff}^{2/11}N_A^{1/11}$	$N_A^{6/11}\nu_{eff}^{1/11}(N_B\tau_B^2)^{2/11}$
$CC1_{qn}$	$N_B^2\tau_B^{8/5}/\nu_A^{6/5}N_A^{9/5}$	$[(\alpha_b\Phi_{ion}/(1-\alpha_b)]^{1/2} \times [(N_A\nu_A^{3/2}/\tau_B^2)]^{1/5}$	$N_B\tau_B^{1/5}/\nu_A^{2/5}N_A^{3/5}$	$N_A^{4/5}\nu_A^{1/5}\tau_B^{2/5}$
$CC1_{os}$	$\{[\alpha_b/(1-\alpha_b)](N_A\Phi_{ion}/\tau_B^2)\}^2$	$(N_B^2\tau_B^{16}/N_A^9) \times \{[(1-\alpha_b)/\alpha_b\Phi_{ion})\}^6$	$(N_B\tau_B^5/N_A^3) \times [(1-\alpha_b)/\alpha_b\Phi_{ion})]^2$	$N_A^2(\Phi_{ion}/\tau_B^2)[\alpha_b/(1-\alpha_b)]$
$CC1_{ch}$	$N_B^2\tau_B^{8/5}/\nu_{eff}^{6/5}N_A^{9/5}$	α_b	$N_B\tau_B^{1/5}/N_A^{3/5}\nu_{eff}^{2/5}$	$N_A^{4/5}\nu_{eff}^{1/5}\tau_B^{2/5}$
$CC2_{qn}$	$N_B\tau_B^2$	$\{[(\alpha_b/(1-\alpha_b)] \times \Phi_{ion}N_B^{1/3}\tau_B^{4/3})\}^{2/3}$	$N_B^{2/3}\tau_B^{1/3}$	$N_A\nu_A^{1/3}N_B^{-1/9}\tau_B^{4/9}$
$CC2_{os}$	$N_B\tau_B^2$	$\{[(\alpha_b/(1-\alpha_b)] \times \Phi_{ion}N_B^{1/3}/\tau_B^{4/3})\}^{2/3}$	$N_B^{2/3}\tau_B^{1/3}$	$(N_A\nu_A^{1/3})[(\alpha_b\Phi_{ion}N_B^{1/3}\tau_B^{-4/3})]^{1/3}$
$CC2_{ch}$	$N_B\tau_B^2$	α_b	$N_B^{2/3}\tau_B^{1/3}$	$N_A\nu_{eff}^{1/3}N_B^{-1/9}\tau_B^{4/9}$

Table 2. Critical Micellar Concentrations

regions	ln cmc + $(N_B\tau_B^2)^{2/3}$
M	
S_{ch}, $S_{qn'}$	$N_A^{1/11}\nu_{eff}^{2/11}(N_B\tau_B^2)^{4/11}$
S_{qn}	$-N_A\ln(1-\alpha_b) + N_A^{1/11}\nu_A^{2/11}(N_B\tau_B^2)^{4/11}$
$CC1_{qn}$	$-N_A\ln(1-\alpha_b) + N_A^{3/5}\nu_A^{2/5}\tau_B^{4/5}$
$CC1_{ch}$, $CC1_{qn'}$	$N_A^{3/5}\nu_{eff}^{2/5}\tau_B^{4/5}$
$CC1_{os}$	$-N_A\ln(1-\alpha_b) + N_A^3(\Phi_{ion}\alpha_b)^2\tau_B^{-4}$
$CC2_{qn}$	$-N_A\ln(1-\alpha_b) + (N_B\tau_B^2)^{1/3} + N_A\nu_A^{2/3}N_B^{-2/9}\tau_B^{8/9}$
$CC2_{os}$	$-N_A\ln(1-\alpha_b) + (N_B\tau_B^2)^{1/3} - N_A(\alpha_b\Phi_{ion}N_B^{1/3}\tau_B^{-4/3})^{2/3}$
$CC2_{ch}$, $CC2_{qn'}$	$(N_B\tau_B^2)^{1/3} + N_A\nu_{eff}^{2/3}N_B^{-2/9}\tau_B^{8/9}$

Table 3. Boundaries of the Regions in the Phase Diagrams (Figures 3)

regions	boundary
S_{ch}−M	$\Phi_{ion} \cong \alpha_b^2N_A^{1/2}(N_B\tau_B^2)^{-5/3}$
S_{ch}−S_{qn}	$\Phi_{ion} = \Phi^*_{ion} \cong \alpha_b^{-7/2}(N_B\tau_B^2)^2N_A^{-5}$
S_{ch}−$S_{qn'}$	$\Phi_{ion} \cong \alpha_b^2/\nu_A$
S_{qn}−M	$\alpha_b \cong N_A^{-4/3}(N_B\tau_B^2)^{2/3}$
S_{qn}−$S_{qn'}$	$\Phi_{ion} \cong \alpha_b(N_B\tau_B^2)^{4/11}N_A^{-10/11}\nu_A^{-9/11}$
S_{ch}−$CC1_{os}$	$\Phi_{ion} = \Phi^*_{ion} \cong \alpha_b^{-7/2}(N_B\tau_B^2)^2N_A^{-5}$
S_{ch}−$CC1_{ch}$	$\Phi_{ion} \cong \alpha_b^2N_A^{7/3}\tau_B^{1/3}N_B^{-5/3}$
$CC1_{ch}$−$CC1_{qn'}$	$\Phi_{ion} \cong \alpha_b^2/\nu_A$
$CC1_{ch}$−$CC1_{os}$	$\Phi_{ion} \cong \tau_B^2(N_A\alpha_b^{1/2})^{-1}$
$CC1_{os}$−$CC1_{qn}$	$\Phi_{ion} \cong \tau_B^{12/5}\nu_A^{1/5}(N_A^{6/5}\alpha_b)^{-1}$
$CC1_{qn}$−$CC1_{qn'}$	$\Phi_{ion} \cong \alpha_b\tau_B^{4/5}(N_A\nu_A^{3/2})^{-2/5}$
$CC2_{qn}$−$CC2_{os}$	$\Phi_{ion} \cong \nu_A\tau_B^{8/3}(\alpha_bN_B^{2/3})^{-1}$
$CC2_{os}$−$CC2_{ch}$	$\Phi_{ion} \cong \alpha_b^{1/2}\tau_B^{4/3}N_B^{-1/3}$
$CC2_{ch}$−$CC2_{qn'}$	$\Phi_{ion} \cong \alpha_b^2/\nu_A$
$CC2_{os}$−$CC1_{os}$	$\Phi_{ion} \cong \tau_B^{7/3}N_B^{1/6}(\alpha_bN_A^{3/2})^{-1}$
$CC1_{ch}$−$CC2_{ch}$	$\Phi_{ion} \cong \alpha_b^2\tau_B^{1/3}N_A^{3/2}N_B^{-5/6}$
$CC2_{qn}$−$CC2_{qn'}$	$\Phi_{ion} \cong \alpha_b^{1/2}N_B^{-1/3}\tau_B^{4/3}$

To the right of the dashed line, the cmc_{qn} is shifted according to eq 38.

In region S_{ch}, the corona blocks are charged, $\alpha \approx \alpha_b$, and the parameters of equilibrium micelles are given by eqs 40−42. The bold line separating regions S_{ch} and S_{qn} is the line of abrupt rearrangement of the micelles, $\Phi_{ion} = \Phi^*_{ion}(\alpha_b)$. In region $S_{qn'}$ the corona blocks are ionized, $\alpha \approx \alpha_b$, but the electrostatic interactions are strongly screened due to high salt concentration. As a result, the structural parameters of the micelles are the same as in region S_{qn}.

Finally, in region M the micelles are unstable, and only free ionized chains (with $\alpha = \alpha_b$) are found in the solution for any polymer concentration. The power law dependences for the micelle parameters and the cmc's are summarized in Tables 1 and 2. The equations for boundaries between various regions of the diagram of states are collected in Table 3. In Figure 5a we present schematically the evolution of the aggregation number and radius of the corona for the star like micelles upon variation of salt concentration.

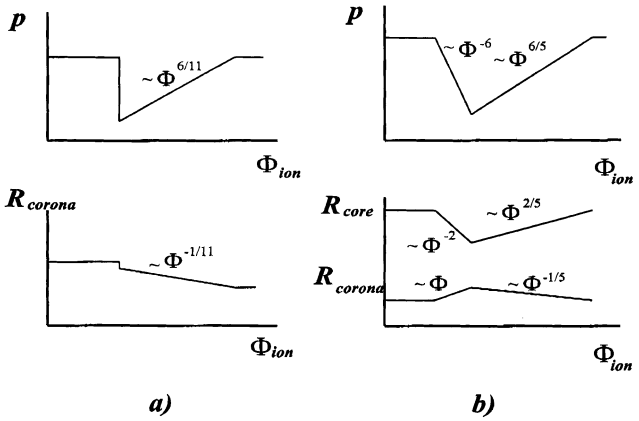

Figure 5. Schematic dependence of the aggregation number and radius of the corona on the salt concentration for starlike (a) and crew-cut 1 (b) micelle.

5. Crew-Cut Polyelectrolyte Micelles

The crew-cut micelles with $R_{corona} \ll R_{core}$ are formed by copolymers with comparatively long hydrophobic blocks. The corona of a crew-cut polyelectrolyte micelle can be viewed as a quasi-planar polyelectrolyte brush, as long as $R_{core} \gg R_{corona}$. The ionization−recombination balance and the structural properties of a planar polyelectrolyte brush were discussed in detail in ref 20. Here, we focus on evolution of crew-cut micelles caused by an increase in the bulk salt concentration Φ_{ion}.

By expanding eq 25 with respect to parameter $N_A\tau_B/N_Bc_p \ll 1$, we find that with the accuracy of numerical coefficients

$$\frac{F}{N_Ak_BT} \simeq \frac{\tau_B^{2/3}N_B^{1/3}}{N_A}\left\{1 + \frac{N_A\tau_B^2}{N_Bc_p^2}\right\}^{1/3} + \nu_Ac_p + \ln(1-\alpha) - \frac{\Phi_{ion}}{c_p}(\sqrt{1 + (\alpha c_p/\Phi_{ion})^2} - 1) \quad (50)$$

Depending on the ratio $N_A\tau_B^2/N_Bc_p^2$, we distinguish two different types of crew-cut micelles. When $N_A\tau_B^2/N_Bc_p^2 \gg 1$, the stretching of blocks A in the corona still dominates over the stretching of blocks B in the core. As a result, the equilibrium parameters of such micelles are determined by the balance of the free energy of the corona and the surface free energy of the core. We refer to such micelles as crew-cut-1 (CC1) micelles. When, however, $N_A\tau_B^2/N_Bc_p^2 \ll 1$, the stretching of blocks B dominates, and the equilibrium parameters of such micelles are determined by the balance of the free energy of the core and the surface free energy. We refer to such micelles as crew-cut-2 (CC2) micelles.

5.1. CC1 Micelles. We start with moderately asymmetric block copolymers with relatively long block A so that

$$N_B^{5/9} v_A^{-2/3} \tau_B^{-2/9} < N_A < N_B^{5/7} v_A^{-3/7} \tau_B^{-1/7} \quad (51)$$

Inequalities 51 ensure that $R_{core} > R_{corona}$, and the stretching of blocks A dominates over the stretching of blocks B in both low/high salt regimes. By retaining the second term in figure brackets in eq 50, we find for the free energy of CC1 micelle

$$\frac{F}{N_A k_B T} \simeq \frac{\tau_B^{4/3}}{N_A^{2/3} c_p^{2/3}} + v_A c_p + \ln(1-\alpha) - \frac{\Phi_{ion}}{c_p}\left(\sqrt{1 + (\alpha c_p/\Phi_{ion})^2} - 1\right) \quad (52)$$

In the low-salt limit, $\Phi_{ion} \ll \alpha_b c_p$, the corona chains are weakly ionized. The degree of ionization, α, progressively increases with increasing concentration of salt; see eq 16. Making use of eq 17.1, we can represent the free energy, eq 52, as

$$F(\alpha)/N_A k_B T \cong -\alpha + \ln(1-\alpha) + v_A c_p + \left(\frac{\tau_B^2}{N_A}\right)^{2/3} c_p^{-2/3} \quad (53)$$

By expanding $\ln(1-\alpha) \approx -\alpha$ and using eq 16 which relates c_p to α, we finally represent the free energy, eq 53, as a function of a single variable α:

$$F(\alpha)/N_A k_B T \cong -2\alpha + v_A \frac{\alpha_b}{1-\alpha_b}\frac{\Phi_{ion}}{\alpha^2} + \left(\frac{1-\alpha_b}{\alpha_b}\frac{\tau_B^2}{N_A \Phi_{ion}}\right)^{2/3} \alpha^{4/3} \quad (54)$$

At low salt concentration the ionization of the corona is suppressed, and the first term in eq 54 is negligible. The structure of micelles is determined by the competition of steric repulsions (the second term) and the excess free energy of the core interface (the last term) to give

$$\alpha \cong \left(\frac{\alpha_b \Phi_{ion}}{1-\alpha_b}\right)^{1/2}\left(\frac{N_A v_A^{3/2}}{\tau_B^2}\right)^{1/5} \quad (55)$$

By using eqs 16.1, 21, and 23, we find the equilibrium parameters of the quasi-neutral CC1 micelle,

$$p_{eq} \cong \frac{N_B^2 \tau_B^{8/5}}{v_A^{6/5} N_A^{9/5}} \quad (56)$$

$$R_{corona} \cong N_A^{4/5} v_A^{1/5} \tau_B^{2/5} \quad (57)$$

$$R_{core} \cong \frac{N_B \tau_B^{1/5}}{v_A^{2/5} N_A^{3/5}} \quad (58)$$

These dependences coincide with those for a micelle formed by a nonionic AB diblock copolymer (in the mean-field approximation). The condition

$$\frac{N_B}{N_A^{7/5} v_A^{3/5} \tau_B^{1/5}} \gg 1 \quad (59)$$

ensures that $R_{core} \gg R_{corona}$, i.e., that the quasi-neutral micelles have the crew-cut shape. As we see below, an increasingly important contribution of the electrostatic interactions in the intermediate range of salt concentration leads to a decrease of the ratio R_{core}/R_{corona}.

As long as the salt concentration remains sufficiently low,

$$\Phi_{ion} \ll \Phi_{ion}^{(1)} \equiv \frac{1-\alpha_b}{\alpha_b}\left(\frac{\tau_B^2}{N_A}\right)^{6/5} v_A^{1/5}$$

an increase in Φ_{ion} does not affect appreciably the structure of the micelles but leads to increasing degree of ionization of the coronal blocks according to eq 55.

An increase in salt concentration promotes the ionization of the corona blocks, and as a result, the first term in eq 54 begins to dominate over the steric repulsion at $\Phi_{ion} \geq \Phi_{ion}^{(1)}$. The structure of the equilibrium micelle is now determined by the balance between the osmotic pressure of counterions in the corona and the excess interfacial free energy of the core. The degree of ionization of the A-blocks in the equilibrium micelle now increases with the salt concentration as

$$\alpha \cong \left(\frac{\alpha_b}{1-\alpha_b}\frac{N_A \Phi_{ion}}{\tau_B^2}\right)^2 \quad (60)$$

With increasing degree of ionization of A-blocks the osmotic repulsion in the corona increases, and therefore, the aggregation number rapidly decreases as

$$p_{eq} \cong \frac{N_B^2 \tau_B^{16}}{N_A^9}\left(\frac{1-\alpha_b}{\alpha_b \Phi_{ion}}\right)^6 \quad (61)$$

Here, the micellar corona is equivalent to a quasi-planar polyelectrolyte brush in the annealing osmotic regime.[20] The extension of the coronal chains is therefore given by

$$R_{corona} \cong \alpha^{1/2} N_A \cong N_A^2 \frac{\Phi_{ion}}{\tau_B^2}\frac{\alpha_b}{1-\alpha_b} \quad (62)$$

i.e., increases with increasing salt concentration, while the size of the core

$$R_{core} \cong \frac{N_B \tau_B^5}{N_A^3}\left(\frac{1-\alpha_B}{\alpha_b \Phi_{ion}}\right)^2 \quad (63)$$

decreases with increasing salt concentration due to a decrease in the aggregation number (eq 61). As a result, the ratio R_{core}/R_{corona} decreases with increasing salt concentration as $\sim 1/(\Phi_{ion})^3$.

The annealing osmotic regime holds as long as $\alpha \ll \alpha_b$, i.e., in the range of the salt concentration $\Phi_{ion} \ll \Phi_{ion}^{(2)}$ where the crossover value is given by

$$\Phi_{ion}^{(2)} \equiv \tau_B^2 \alpha_B^{-1/2} (1-\alpha_b)^{5/6} N_A^{-1} \quad (64)$$

At $\Phi_{ion} \cong \Phi_{ion}^{(2)}$ the blocks A in the corona reach the maximal degree of ionization, $\alpha \approx \alpha_b$, and the maximal extension, $R_{corona} \cong \alpha_b^{1/2} N_A$. On the contrary, the aggregation number reaches its minimal value and is

equal to

$$p_{\Phi_{ion}^{(2)}} \cong \frac{(N_B\tau_B^2)^2}{(\alpha_b N_A)^3}$$

(Note that $p_{\Phi_{ion}^{(2)}}$ coincides with the aggregation number for a quenched polyelectrolyte micelle with $\alpha = \alpha_b$ in a salt-free solution.[15−17]) The ratio R_{core}/R_{corona} also passes through a minimum at $\Phi_{ion}^{(2)}$:

$$\left(\frac{R_{core}}{R_{corona}}\right)_{min,\Phi_{ion}^{(2)}} \cong \frac{N_B\tau_B}{N_A^2\alpha_b^{3/2}} \quad (65)$$

At larger salt concentrations, $\Phi_{ion} \gg \Phi_{ion}^{(2)}$; the corona is found in the salt dominance regime. Here, $\alpha_b c_p/\Phi_{ion} \ll 1$, and the free energy of the micelle, eq 52, is given by

$$F(c_p)/N_A k_B T \cong \ln(1-\alpha_b) + c_p\left(v_A + \frac{\alpha_b^2}{\Phi_{ion}}\right) + \left(\frac{\tau_B^2}{N_A}\right)^{2/3} c_p^{-2/3} \quad (66)$$

With increasing salt concentration the electrostatic interactions in the corona get progressively screened while the degree of dissociation of the coronal blocks remains virtually unaffected (it weakly increases according to eq 16.2). As a result, the aggregation number in the optimal micelle (corresponding to the minimum of the free energy, eq 66), increases as

$$p_{eq} \cong \frac{N_B^2\tau_B^{8/5}}{(v_A + \alpha_b^2/\Phi_{ion})^{6/5} N_A^{9/5}} \quad (67)$$

together with the core radius

$$R_{core} \cong \frac{N_B\tau_B^{1/5}}{N_A^{3/5}}\left(v_A + \frac{\alpha_b^2}{\Phi_{ion}}\right)^{-2/5} \quad (68)$$

while the span of the corona weakly decreases as

$$R_{corona} \cong N_A^{4/5}\left(v_A + \frac{\alpha_b^2}{\Phi_{ion}}\right)^{1/5} \tau_B^{2/5} \quad (69)$$

In the range of salt concentrations $\Phi_{ion}^{(2)} \ll \Phi_{ion} \ll \alpha_b^2/v_A$ the electrostatic contribution to the v_{eff} dominates over the steric one, and $v_{eff} = v_A + \alpha_b^2/\Phi_{ion} \cong \alpha_b^2/\Phi_{ion}$. At higher salt content, $\Phi_{ion} \gg \alpha_b^2/v_A$, the electrostatic interactions get screened off, and the micelles are found in the quasi-neutral regime, described by eqs 56−68.

The described scenario of the continuous rearrangement of micelles upon variation in the ionic strength holds if $R_{corona} \ll R_{core}$ in the whole range of the salt concentrations (including $\Phi_{ion}^{(2)}$, where R_{core} and R_{corona} reach their minimal and maximal values, respectively).

The condition $R_{corona} \ll R_{core}$ can, however, break down at relatively high values of $\alpha_b > N_B^{2/3}\tau_B^{2/3}N_A^{-4/3}$. In this range of α_b, the stronger electrostatic interactions in the corona transform CC1 micelles into starlike micelles when bulk concentration of salt reaches the value of $\Phi_{ion} = \Phi_{ion}^*$ (eq 48). This rearrangement occurs abruptly (as the first-order phase transition) when the coronae of CC1 micelles swell in the osmotic regime ($\Phi_{ion} > \Phi_{ion}^{(1)}$). The equilibrium parameters of the micelles after the transition coincide with those for charged starlike micelles (eqs 40−32).

Our results for CC1 micelles are summarized in the diagram of the states in Figure 3b. One finds here regions $CC1_{qn}$, $CC1_{qn'}$, $CC1_{osm}$, $CC1_{ch}$, and S_{ch}. In region $CC1_{qn}$ the micelles are quasi-neutral. (The dashed line indicates the value of α_b above which the cmc_{qn} deviates from cmc_n according to eq 38.) Line $\Phi_{ion}^{(1)}$ separates regions $CC1_{qn}$ and $CC1_{osm}$. In region $CC1_{osm}$ the coronae of micelles swell due to increasing ionization of the chains. The bold line indicates the transition line $\Phi_{ion} = \Phi_{ion}^*(\alpha_b)$ where weakly ionized osmotic crew-cut micelles abruptly transform into strongly charged starlike micelles (region S_{ch}). In region $CC1_{ch}$ the charged micelles acquire a crew-cut shape. Line $\Phi_{ion}^{(2)}$ separates regions $CC1_{osm}$ and $CC1_{ch}$. Crossing this line does not lead to abrupt transformation of micelles.

The evolution of the aggregation number, the degree of dissociation, and the extension of the coronal chains in a crew-cut micelle with increasing salt concentration are schematically presented in Figure 5b.

5.1.1. Cmc for Crew-Cut-1 Micelles. By using eqs 3 and 35 and the corresponding expressions for micelle free energies, we find cmc for all the regimes of CC1 micelles. The results are summarized in Table 3. We emphasize that, in contrast to the nonmonotonic behavior of equilibrium parameters of CC1 micelles, the cmc decreases monotonically as bulk salt concentration Φ_{ion} increases, namely

$$\ln(cmc)_{CC1} \cong \begin{cases} \text{const} - N_A^3(\alpha_b\Phi_{ion}/\tau_B^2(1-\alpha_b)), & \Phi_{ion} \ll \Phi_{ion}^{(2)} \\ \text{const}' + N_A^{3/5}\tau_B^{4/5}(v_A + \alpha_b^2/\Phi_{ion})^{2/5}, & \Phi_{ion} \gg \Phi_{ion}^{(2)} \end{cases} \quad (70)$$

5.2. CC2 Micelles. When the length of insoluble block B is large enough so that

$$N_B^{5/9} v_A^{-2/3} \tau_B^{-2/9} > N_A \quad (71)$$

the stretching of blocks B in the core dominates over the free energy of the corona in low/high salt regimes. Here, $N_A\tau_B^2/N_B c_p^2 \ll 1$, and the second term in square brackets in eq 50 can be safely omitted. The free energy of micelle is then given by

$$\frac{F}{N_A k_B T} \simeq \frac{\tau_B^{2/3} N_B^{1/3}}{N_A} + v_A c_p + \ln(1-\alpha) - \frac{\Phi_{ion}}{c_p}\left(\sqrt{1 + (\alpha c_p/\Phi_{ion})^2} - 1\right) \quad (72)$$

where α is related to c_p via eq 15. Here, radius of the core (eq 23)

$$R_{core} \simeq \tau_B^{1/3} N_B^{2/3} \quad (73)$$

and the aggregation number

$$p_{eq} \simeq \frac{R_{core}^3\tau_B}{N_B} \simeq \tau_B^2 N_B \quad (74)$$

do not depend on α_b and Φ_{ion}, and the corona of micelle constitutes a quasi-planar ionizable brush with area $s \simeq R_{core}^2/p \simeq N_B^{1/3}\tau_B^{-4/3}$ per chain. The parameters of the corona, α and R_{corona}, are, therefore, given by the

corresponding expressions for an annealing planar brush. Namely, in a quasi-neutral (dominance of nonelectrostatic interactions in the corona) regime

$$R_{corona} \simeq N_A {v_A}^{1/3} s^{-1/3} \simeq N_A {v_A}^{1/3} {N_B}^{-1/9} {\tau_B}^{4/9} \quad (75)$$

$$\alpha \simeq (\alpha_b \Phi_{ion} {N_B}^{1/3} {\tau_B}^{-4/3})^{2/3} \quad (76)$$

and

$$F/N_A k_B T \simeq \frac{{\tau_B}^{2/3} {N_B}^{1/3}}{N_A} + {v_A}^{2/3} {\tau_B}^{8/9} {N_B}^{-2/9} \quad (77)$$

In an annealing osmotic regime for the corona (that starts when salt concentration $\Phi_{ion} > \alpha_b^{-1} v_A N_B^{-2/3} \tau_B^{8/3}$), the height of corona is given by

$$R_{corona} \simeq N_A \alpha^{1/2} \simeq N_A {v_A}^{1/3} (\alpha_b \Phi_{ion} {N_B}^{1/3} {\tau_B}^{-4/3})^{1/3} \quad (78)$$

whereas α increases with an increase in Φ_{ion} according to eq 76. Here, the free energy in equilibrium micelle is given by

$$F/N_A k_B T \simeq \frac{{\tau_B}^{2/3} {N_B}^{1/3}}{N_A} - (\alpha_b \Phi_{ion} {N_B}^{1/3} {\tau_B}^{-4/3})^{2/3} \quad (79)$$

In the high salt regime (which starts when $\Phi_{ion} > \Phi_{ion}^{(2)}$), the degree of ionization approaches its bulk value, $\alpha \approx \alpha_b$, and the radius of the corona is given by

$$R_{corona} \simeq \left(v_A + \frac{{\alpha_b}^2}{\Phi_{ion}}\right)^{1/3} N_A (s)^{-1/3} \simeq \left(v_A + \frac{{\alpha_b}^2}{\Phi_{ion}}\right)^{1/3} N_A {N_B}^{-1/9} {\tau_B}^{4/9} \quad (80)$$

The equilibrium free energy of the micelle yields

$$F/N_A k_B T \simeq \frac{{\tau_B}^{2/3} {N_B}^{1/3}}{N_A} + \left(v_A + \frac{{\alpha_b}^2}{\Phi_{ion}}\right)^{2/3} {N_B}^{-2/9} {\tau_B}^{8/9} + \ln(1 - \alpha_b) \quad (81)$$

The described scenario holds for weakly charged polymers ($\alpha_b < {N_B}^{1/3} {\tau_B}^{2/3} {N_A}^{-1}$). Such copolymers form CC2 micelles in the whole range of Φ_{ion}. When $\alpha_b > {N_B}^{1/3} {\tau_B}^{2/3} {N_A}^{-1}$, an increase in salt concentration can transform CC2 micelle into CC1 micelle. The corresponding diagram of the states is presented in Figure 3c.

5.2.1. Cmc for Crew-Cut-2 Micelle. Following the same lines, we calculate the critical micelles concentrations for all the delineated regimes. The cmc_{CC2} follows the same trends as cmc_{CC1}. The results are summarized in Table 3.

6. Discussion and Conclusions

We developed a mean-field theory which describes micellization in solutions of diblock copolymers with one hydrophobic and one weakly dissociating (annealing) polyelectrolyte block.

In framework of this model we obtained the power law dependences for the equilibrium parameters of spherical micelles (the aggregation number, the corona, and the core sizes) and for the cmc as a function of molecular weights of the blocks, N_A and N_B, and of the pH (via α_b) and the ionic strength in the bulk solution. Our previous results (ref 17) indicate that for micelles with quenched polyelectrolyte blocks the exponents yielding from the mean-field theory are slightly different from the values predicted by the consistent scaling model. However, the quantitative difference between the mean-field and the scaling exponents is almost below the accuracy of any experimental measurement. At the same time, all main qualitative trends in the behavior of the system are correctly described by the mean-field theory. We therefore believe that our simple model captures the main features of micelles with annealing polyelectrolyte blocks as well.

As was demonstrated earlier (ref 17), in the case of block copolymers with quenched polyelectrolyte blocks the addition of salt to the micellar solution leads to (i) decreasing cmc, (ii) increasing aggregation number in the equilibrium micelles, and (iii) weak decrease in the span of the micellar corona formed by polyelectrolyte chains. The physical origin of these effects is progressive screening of the Coulomb repulsive interaction in the micellar coronae upon an increase in the salt concentration.

The general picture of salt-induced evolution of the annealed polyelectrolyte micelles is dramatically different from that for the quenched polyelectrolytes micelles and is more complicated. An increase in salt concentration leads not only to screening of the Coulomb interactions but also to the enhanced ionization of the polyelectrolyte blocks in the corona. The latter effect is analogous to salt-induced ionization of polyelectrolyte chains in polyelectrolyte brushes[20] and the coronae or star-branched polyelectrolytes.[21,22]

However, in a marked contrast to brushes and starlike polymers, the ionization−recombination equilibrium in annealing micelle is coupled to the association−dissociation self-assembly. As a result, an increase in salt concentration leads to the nonmonotonic variation in the aggregation number and in other structural parameters of the equilibrium micelles.

At low (vanishing) salt concentration (and sufficiently low pH, i.e., small α_b) large quasi-neutral micelles are formed. Because of high polymer density in the corona the ionization of blocks A is strongly suppressed, and the corona is fairly noncharged. In this regime the growth of micelles is opposed by the nonelectrostatic (steric) repulsion between monomers, and the micelles have the same structure as nonionic block copolymer aggregates.

An increase in the bulk salt concentration leads to progressive ionization of the corona blocks due to release of hydrogen ions from the corona and their substitution by sodium ions. (cf. refs 20−22). As a result, osmotic repulsion between the corona blocks gets stronger. This, in turn, leads to the decrease in aggregation number and simultaneous increase in the radius of the corona.

For crew-cut micelles with long insoluble block B the decrease in aggregation number upon an increase in the salt concentration occurs continuously. Here, an increase in osmotic repulsion in the corona is balanced by a corresponding increase in the excess free energy of the core interface until corona blocks reach the maximal degree of ionization, $\alpha = \alpha_b$.

In contrast to crew-cut micelles, in starlike micelles a decrease in the aggregation number is accompanied by such strong enhancement in the osmotic repulsion in the corona that it cannot be balanced by an increase

in the free energy of core interface. As a result, at certain critical salt concentration Φ^*_{ion}, the quasi-neutral starlike micelles become unstable and dissociate into smaller ones, in which the corona blocks are ionized up to $\alpha \approx \alpha_b$. The same transformation can happen also for crew-cut micelles with short insoluble block B. In framework of our mean-field model, the jump-wise rearrangements of micelles occur as the first-order phase transitions.

Further evolution of micelles upon an increase in the salt concentration is similar to evolution of micelles with quenched blocks with $\alpha = \alpha_b$ (i.e., the aggregation number increases whereas the extension of the corona blocks decreases due to enhancing screening of the electrostatic interactions by added salt).

An increase in pH (i.e., in α_b) leads to increasing ionization of the coronal chains and, as a result, to decreasing aggregation number. Both occur either continuously or abruptly (the latter is the case if the line $\Phi^*_{ion}(\alpha_b)$ is crossed).

Altogether, we predict a nonmonotonic variation of all the structural parameters of the equilibrium micelles as a function of salt concentration: the aggregation number passes through a minimum, while the span of the micellar corona passes through a maximum. This evolution is either continuous (in the case of crew-cut-2 micelles and weakly charged crew-cut-1 micelles) or discontinuous (for starlike micelles and strongly charged crew-cut-1 micelles). In the latter case we expect abrupt decomposition of large quasi-neutral micelles into smaller strongly ionized ones and the coexistence of small and large micelles in a narrow range of salt concentrations. The degree of ionization of blocks A in the corona increases upon an increase in the bulk salt concentration either continuously or with a upward jump depending on the type of micelle rearrangement (continuous vs abrupt scenario).

The described above charge "annealing" effects are expected to be important for low or moderate pH < p*K*, while at high pH blocks A are strongly ionized, $\alpha \cong \alpha_b$, and the behavior of block copolymers with quenched polyelectrolyte blocks is recovered. At low salt concentration an increase in pH from pH < p*K* to pH > p*K* affects considerably Φ_{ion}; i.e., ionization is partially suppressed in the neutral range of pH (cf. ref 22).

Verification of our theory is a challenging experimental problem. A proper choice of block copolymer would be of crucial importance here. The predicted effects of nonmonotonic variations in micelle parameters and jump-wise transitions are inherently linked to equilibration of micelle structure. Therefore, "popular" block copolymers with PS as a hydrophobic block would not work here. A number of experimental observations suggest that due to high T_g of PS, the micelles with PS core are essentially nonequilibrium. (They do not rearrange in response to variations in the ionic strength in the solution or temperature.) Copolymers with "softer" hydrophobic block (such as, e.g., PtBS) are more suitable candidates to produce the equilibrium micelles. Recent experiments of Forster et al.[8] performed on PSS/PtBS copolymers (starlike micelles with quenched polyelectrolyte blocks) demonstrated a good agreement between the predicted[17] and measured exponents for micelle hydrodynamic radius vs salt concentration dependence. This observation seems to indicate the equilibrium nature of micelles comprising PtBS core block. Therefore, copolymers that have PtBS hydrophobic block linked to a weak polyelectrolyte block (e.g., PAA, PMAA, PVP, etc.) could be promising candidates to check our theory.

As emphasized earlier, the salt-induced nonmonotonicity in micelle characteristics is coupled to the enhancement of corona ionization. This ionization "flexibility" could add a novel pattern in the interfacial behavior of annealing polyelectrolyte micelles. In particular, a charged interface would enhance ionization of an oppositely charged micelle. Because of a decrease in co-ion concentration near the interface, such a micelle is found under effectively different pH promoting extra ionization of the corona blocks. As a result, the charge on the interface can trigger abrupt transformations of micelles with short insoluble blocks and therefore lead to a sophisticated surface pattern. These effects will be considered in a forthcoming publication.

Acknowledgment. E.B.Z. acknowledges the financial support from the National Science Foundation (Grant DMR-9973300). This work has been partially supported by the Dutch National Science Foundation (NWO) program "Self-Organization and Structure of Bionanocomposits" No. 047.009.016.

References and Notes

(1) Kiserow, D.; Prochazka, K.; Ramireddy, C.; Tuzar, Z.; Munk, P.; Webber, S. E. *Macromolecules* **1992**, *25*, 461.
(2) Khougaz, K.; Astafieva, I.; Eisenberg, A. *Macromolecules* **1995**, *28*, 7135.
(3) Amiel, C.; Sikka, M.; Schneider, J. W.; Tsao, Y. H.; Tirrell, M.; Mays, J. W. *Macromolecules* **1995**, *28*, 3125.
(4) (a) Guenoun, P.; Delsanti, M.; Gaseau, D.; Auvray, L.; Cook, D. C.; Mays, J. W.; Tirrell, M *Eur. Phys. J. B* **1998**, *1*, 77. (b) Guenoun, P.; Davis, H. T.; Tirrell, M.; Mays, J. W. *Macromolecules* **1996**, *29*, 3965. (c) Guenoun, P.; Muller, F.; Delsanti, M.; Auvray, L.; Chen, Y. J. Mays, J. W.; Tirrell, M. *Phys. Rev. Lett.* **1998**, *81*, 3872. (d) Muller, F.; Delsanti, M.; Auvray, L.; Yang, J.; Chen, Y. J.; Mays, J. W.; Demé, B.; Tirrell, M.; Guenoun, P. *Eur. Phys. J. E* **2000**, *3*, 45.
(5) Förster, S.; Hemsdorf, N.; Leube, W.; Schnablegger, H.; Regenbrecht, M.; Akari, S.; Lindner, P.; Böttcher, C. *J. Phys. Chem.* **1999**, *103*, 6657.
(6) (a) Groenewegen, W.; Egelhaalf, S. U.; Lapp, A.; van der Maarel, J. R. C. *Macromolecules* **2000**, *33*, 3283. (b) Groenewegen, W.; Lapp, A.; Egelhaalf, S. U.; van der Maarel, J. R. C. *Macromolecules* **2000**, *33*, 4080.
(7) Schuch, H.; Klingler, J.; Rossmanith, P.; Frechen, T.; Gerst, M.; Feldthusen, J.; Müller, A. H. E. *Macromolecules* **2000**, *33*, 3687.
(8) Förster, S.; Hermsdorf, N.; Böttcher, C.; Lindner, P. *Macromolecules* **2002**, *35*, 4096.
(9) Napper, D. H. *Polymeric Stabilization of Colloidal Dispersions*; Academic Press: London, 1985.
(10) *Stealth Liposomes*; Lasic, D., Martin, F., Eds.; CRC Press: Boca Raton, FL, 1995.
(11) Allen, C.; Maysinger, D.; Eisenberg, A. *Colloids Surf. B* **1999**, *16*, 3.
(12) Cammas-Marion, S.; Okano, T.; Kataoka, K. *Colloids Surf. B* **1999**, *16*, 207.
(13) Marko, J. F.; Rabin, Y. *Macromolecules* **1992**, *25*, 1503.
(14) Wittmer, J.; Joanny, J.-F. *Macromolecules* **1993**, *26*, 2691.
(15) Shusharina, N. P.; Nyrkova, I. A.; Khokhlov, A. R. *Macromolecules* **1996**, *29*, 3167.
(16) Huang, C.; Olivera de la Cruz, M.; Delsanti, M.; Guenoun, P. *Macromolecules* **1997**, *30*, 8019.
(17) Borisov, O. V.; Zhulina, E. B. *Macromolecules* **2002**, *35*, 4472.
(18) (a) Halperin, A. *Europhys. Lett.* **1989**, *8*, 351. (b) Halperin, A.; Alexander, S. *Macromolecules* **1989**, *22*, 2403.
(19) Birshtein, T. M.; Zhulina, E. B. *Polymer* **1989**, *30*, 170.
(20) (a) Zhulina E. B.; Birshtein, T. M.; Borisov O. V. *Macromolecules* **1995**, *28*, 1491. (b) Lyatskaya, Yu. V.; Leermakers, F. A. M.; Fleer, G. J.; Zhulina, E. B.; Birshtein, T. M. *Macromolecules* **1995**, *28*, 3562.
(21) Borisov, O. V.; Zhulina, E. B. *Eur. Phys. J. B* **1998**, *4*, 205.

(22) Klein Wolterink, J.; van Male, J.; Cohen Stuart, M.; Koopal, L. K.; Zhulina, E. B.; Borisov, O. V. *Macromolecules*, submitted.
(23) Currie, E. P. K.; Sieval, A. B.; Fleer, G. J.; Cohen Stuart, M. A. *Langmuir* **2000**, *16*, 8324.
(24) Guo, X.; Ballauff, M. *Phys. Rev. E* **2001**, *64*, 05146.
(25) Pincus, P. A. *Macromolecules* **1991**, *24*, 2912.
(26) (a) Borisov O. V.; Birshtein T. M.; Zhulina E. B. *J. Phys. II* **1991**, *1*, 521. (b) Zhulina E. B.; Borisov O. V.; Birshtein T. M. *J. Phys. II* **1992**, *2*, 63. (c) Borisov, O. V.; Zhulina E. B.; Birshtein T. M. *Macromolecules* **1994**, *27*, 4795.
(27) (a) Zhulina, E. B.; Borisov O. V. *J. Chem. Phys.* **1997**, *107*, 5952. (b) Zhulina, E. B.; Klein Wolterink, J.; Borisov, O. V. *Macromolecules* **2000**, *33*, 4945.
(28) Borisov O. V. *J. Phys. II* **1996**, *6*, 1.
(29) Klein Wolterink, J.; Leermakers, F. A. M.; Fleer, G. J.; Koopal, L. K.; Zhulina, E. B.; Borisov, O. V. *Macromolecules* **1999**, *32*, 2365.
(30) (a) Watanabe, H.; Patel, S. S.; Argillier, J. F.; Parsonage, E. E.; Mays, J.; Dan-Brandon, N.; Tirrell, M. *Mater. Res. Soc. Symp. Proc.* **1992**, *249*, 255. (b) Mir, Y.; Auroy, P.; Auvray, L. *Phys. Rev. Lett.* **1995**, *75*, 2863. (c) Guenoun, P.; Schlachli, A.; Sentenac, D.; Mays, J. W.; Benattar, J. J. *Phys. Rev. Lett.* **1995**, *74*, 3628. (d) Ahrens, H.; Förster, S.; Helm, C. A. *Phys. Rev. Lett.* **1999**, 4798.
(31) de Gennes, P. G. *Scaling Concepts in Polymer Physics*, Cornell University Press: Ithaca, NY, 1979.

MA020865S